TWIST and the Analysis of Detector Plane Geometry

Ashley Rose

TRIUMF

4004 Wesbrook Mall

Vancouver, BC

Physics and Astronomy Co-op Work Term Report

in partial fulfillment

of the requirements of the Physics and Astronomy Co-op Program

Summer 2007

Ashley Rose

Department of Physics and Astronomy

University of Victoria

August 31, 2007

Abstract

An algorithm was created to confirm the presence of inclines of drift chamber planes inside the TWIST detector. The program could also determine the shape of the planes. It computed the differences of the drift times for two halves of each plane. This program was used to test for tilting and geometry of these planes using data under different pressures taken in 2004. The geometries were fitted into planar structures and their slopes and constants showed possible tilts in the planes.

Contents

List of Figures

1 Introduction

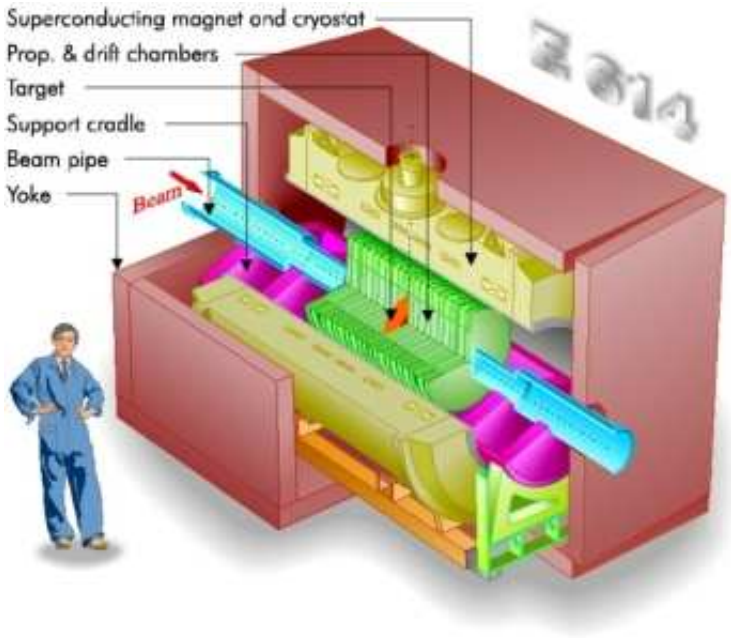

Figure 1: TWIST Spectrometer

The TRIUMF Weak Interaction Symmetry Test, or TWIST (Figure 1), was created to test the energy spectrum of muon decay positrons. Also to see if the behaviour was representative of the theoretical muon spectrum demonstrated in Figure 2.

Beam M13 at TRIUMF sends the polarized positively charged muons through a uniform magnetic field of 2 Tesla. Once the muon beam encounters the 75 μm thick target at the centre of the precision detector, the muons are stopped to rest and decay into a positron and two neutrinos as described in Equation (1),

$$\mu^+ \rightarrow e^+ + \nu_e + \bar{\nu}_\mu \tag{1}$$

The detector (Figure 3) is symmetric in the forward and reverse decay regions to increase sensitivity for measurements. The information provided by the chambers allows for the calculation of the momenta and trajectories of the particles. Helium gas outside the chambers and dimethel ether inside the detector are used to control the pressure and as a result, the bulging. The homogeneous magnetic field in the detector is used to reconstruct the particle's momentum. The particles move in helices inside the detector.

The detector is composed of two types of wire chambers. There are 44 drift chambers (DCs) and 12

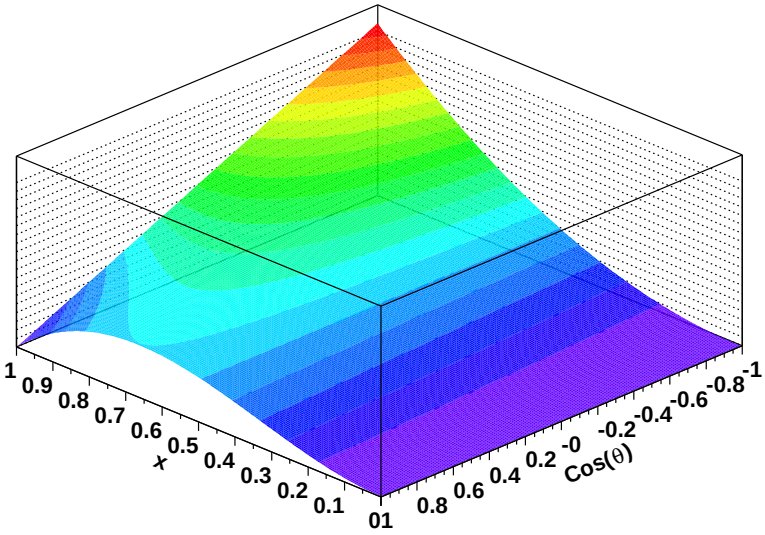

Figure 2: Theoretical Michel Spectrum.

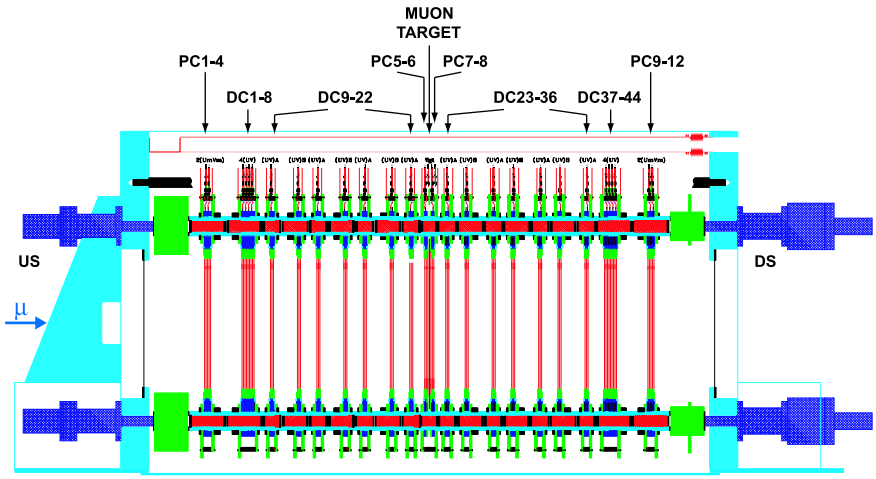

Figure 3: TWIST Detector

proportional chambers (PCs). DC chambers use dimethyl ether (DME) as a gas for its small Lorentz angle. There are 80 gold-plated tungsten anode wires in each DC with a diameter of 15μm. The wires are separated by 4mm. The 6.35 μm thick aluminized Mylar foil walls are, by design, 2mm away from the wires [4]. However, there may be some asymmetry.

The DC chambers record the path of the particles while it travels through the chambers(Figure 4). The DC chambers are further classified as "UV modules" or "dense stack" [4]. UV modules are rotated by $\pm$45 degrees relative to vertical (U planes are tilted +45 degrees and V planes are tilted -45 degrees). Planes in the outside dense stacks have a pattern of V, U, V, U, U, V, U, V. The inner planes follow a U, V, U, V, ... pattern.

PC chambers, on the other hand, use isobutane gas and are used to select events, and not for tracking.

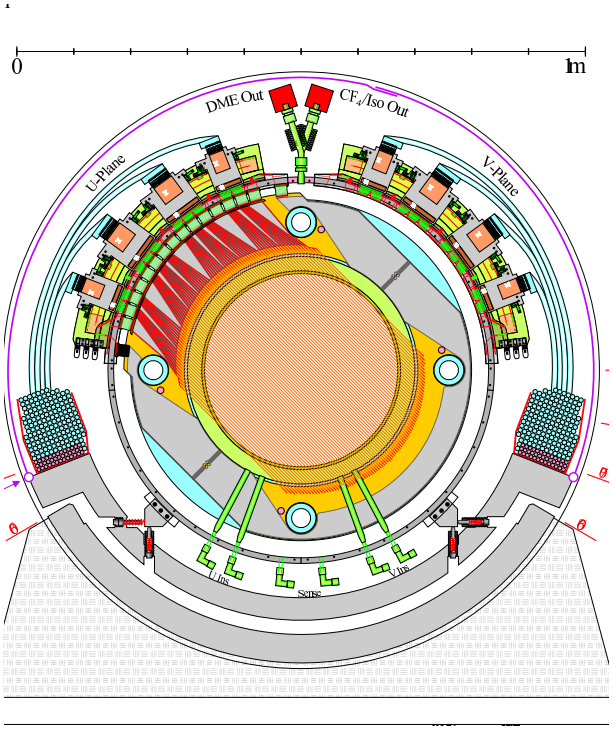

Figure 4: Drift Chamber Planes

Recently, the geometry of the DC planes has come into question. The planes are designed to be flat and exactly perpendicular to the propagation of the muon beam in the detector. Problems arise if the planes have shifted by construction so that they are no longer perpendicular to the muon beam. The software used to analyse this data assumes that the planes are perfectly positioned, but this is

not necessarily the case.

This hypothesis has previously been tested and a large part of this task was to confirm earlier results by Jingliang Hu and compare results with those of Vladimir Selivanov[3], [7]. This report compares its results to the outcomes of two of the earlier works.

2 Determination of Plane Geometry

As previously stated, the intent of this analysis is to validate the existence of possible tilting in the planes and to measure their geometry using only the drift times from 2004 data. The data was used to estimate the distance between foils.

The electric field inside the DCs will affect data under different conditions like pressure. As the wire and cathode plane approach, as would happen if the pressure decreases, the electric field between them gets stronger. A stronger electric field gives the particle a faster acceleration, and leads to shorter drift times. The opposite is also true in that larger pressures spread the wire and cathode plane apart, lowering the electric field between them, and inducing a slower drift time.

Systematic differences in drift times depending on position, chamber, pressure, and temperature would be an indication of a hit.

2.1 Method

Each data set was taken from 2004 data. Different pressures of 77mT, 107mT (data and Monte Carlo), and 137mT were used. Different pressures of the gases inside the detector cause the foils to "bulge".

The data was initially analysed in two ways: once with a tree analysis used with ROOT to test for tilting in the planes, and once using a procedure similar to a previous study done of the 2004 data to validate the analysis by Jingliang Hu. Jingliang's method was also tested to see a concentric bulge using his cuts, disk and ring definitions [3].

All 44 drift chamber planes are considered and further split up into seven U bins, seven V bins, and two Z bins. The purpose of having two Z bins is that the drift time "hit" could occur on either side of the wire. Figure 5 gives an example of a U and a V plane side-by-side and show the position of the wires in the plane. It also demonstrates why it is important to know the side of the wire where the drift time occurs.

The hit can occur in the larger or smaller space between the wire and the foil (the larger side is

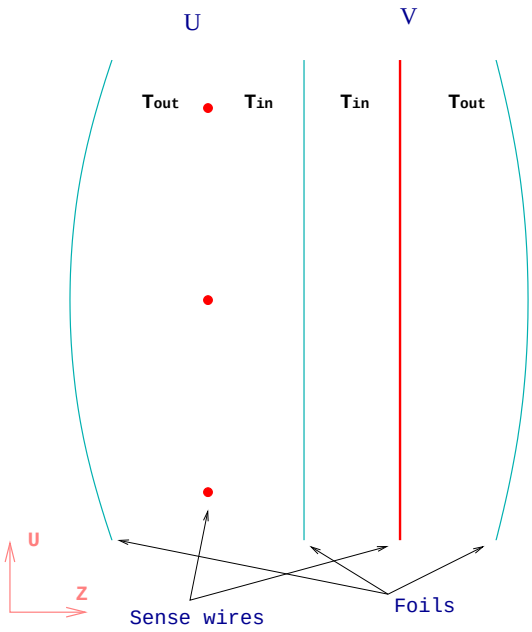

Figure 5: Exaggerated illustration of bulging of DC modules of U and V planes [3].

2.15cm wide and the smaller side is 1.85cm wide), upstream or downstream, and was then classified as being in one of these Z bins. The Z position was determined by the helix-fitter, a program that reconstructs the helical path of the particle from the drift time positions. Different wire/plane distances should then cause systematically different drift time distributions. The means of the bins can be used for measurements. Figure 6 compares the two drift times for DC 28, U bin 6 (2.13cm to 6.39cm), V bin 3 (-6.13cm to -2.16cm), Z bins 1 (smaller space between foil and wire) and 2 (larger space between foil and wire) respectively for nominal data at a pressure of 107mT.

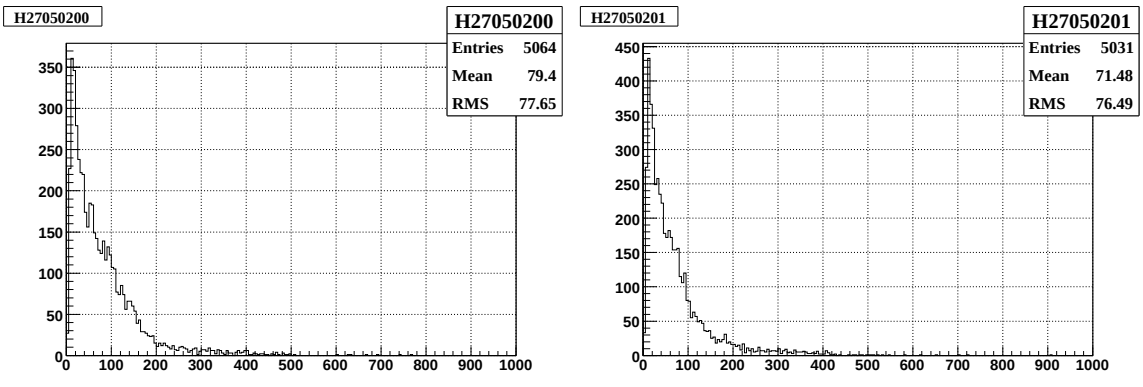

Figure 6: Comparison of drift times for DC 28 (left: z < 0, right: z > 0)

The means of each of the two histograms are used to calculate the difference of each bin. The difference of the means was then filled into the appropriate (U,V) bin in the plane.

$$\mathrm{dt} = \begin{cases} \mathrm{dt}_0 - \mathrm{dt}_1 & \text{if plane number is even} \\ \mathrm{dt}_1 - \mathrm{dt}_0 & \text{if plane number is odd} \end{cases}$$

In the end, there are 44 planes with 49 bins of differences of means of histograms (and their statistical errors). The subtraction changes whether the plane was odd or even (either a V or a U plane) to ensure the proper sign is used for the bulge.

2.2 Validation

Jingliang Hu's study had found that "there is a systematic shift in the cathode foil positions" [3]. In the method based on that by Jingliang, there are two regions (not four like in Figure 7). There was a bin for a disk at the centre and a ring instead of seven u and seven v bins. The disk had a radius of 5cm and the ring spanned the region between 9.5 and 12.5cm (Figure 7).

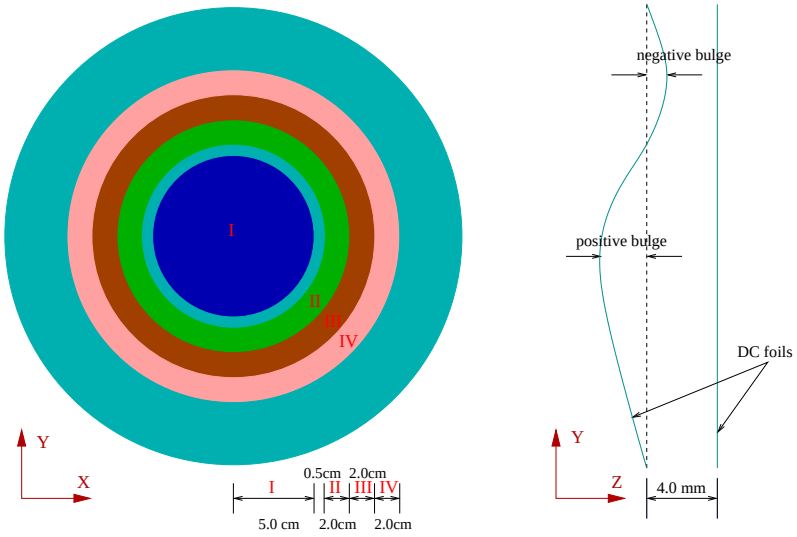

Figure 7: Layout of Plane for Jingliang's Analysis

The other difference was that absolute value of cosine theta values of the drift times are between 0.3 and 0.75.

2.2.1 Pressure of Zero Bulge

The Pressures of Zero Bulge, (Figure 8), plot showed that the average p0 pressure of no bulging was 114.5 ± 2.063 mT. This was consistent with the previous analysis, which found the pressure equal to 115.3 ± 0.7 mT [2]. The smaller error in Hu's result was likely due to the fact that he used six different pressures in his analysis while this one only used three. Thus, his method would have had higher statistics. This plot shows that the observables react to external physical parameters like pressure [2].

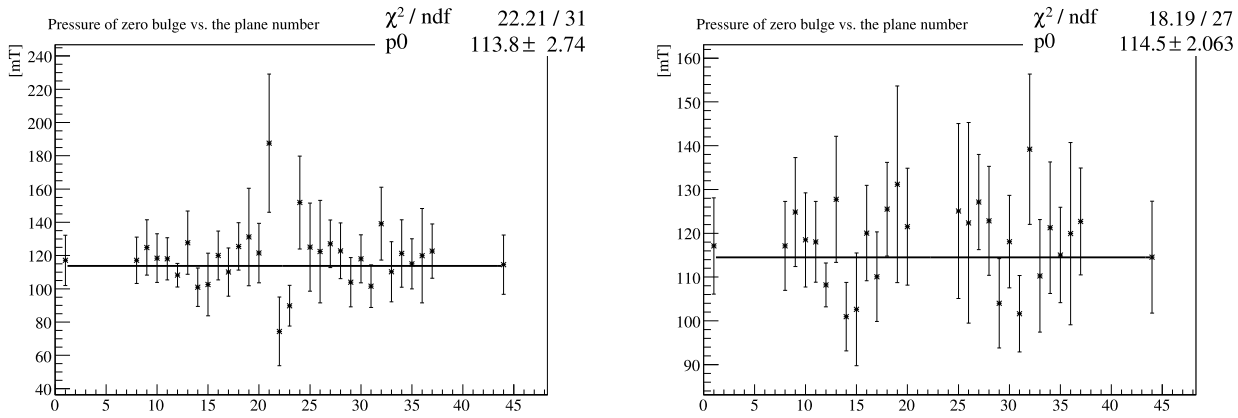

Figure 8: Zero bulge pressures in the planes with and without planes 21-24 respectively.

2.2.2 Fitting the Planes

Each of these 44 sets of data was fitted to planes and their slopes are checked for plane geometry. To see the trend in plane geometry, the U and V slopes, and the constant terms of each plane are plotted against plane number for the U and V planes separately. The slopes and constants are compared with Monte Carlo data. Monte Carlo data must differ from the nominal data to show signs of tilt in the planes. If Monte Carlo data shows the same slopes as the nominal data then there cannot be tilting because there are no tilts in the Monte Carlo data.

Following the fits, the entries are then processed through certain cuts to eliminate less reasonable drift times. Had the drift times not been removed, the helix-fitter would have given badly-reconstructed tracks. In particular, drift times belonging to tracks with momentums under 20MeV are removed. Angle cuts removed drift times that are outside of the range cosine theta between absolute values 0.45 and 0.9. The last cut, the Z cut, made the sides of the wire the same size, since one

side was larger than the other. This Z cut removed drift times less than 0.025cm from the wire and more than 0.18cm from the wire (too close to the foils), effectively making the regions the same size and removing any asymmetry.

2.2.3 Differences of Fits

The fitted slopes of each nominal data are subtracted from the non-fitted data set, leaving residuals. The residuals are always close to zero after the subtraction, which indicates that the tracks are near planar. Figure 9, shows the plots for plane 35 in nominal 107mT data. Clockwise from the top left: raw data plot, fitted plane of the raw data, errors on the raw data (ns), residuals. The electronic version in colour shows the sloping trend clearly .

Another interesting test was to consider each half of the plane before subtracting drift times ($z < 0$, $z > 0$). There are structures in the planes when the difference of these regions is not done, which is a problem. The plots would show horizontal and vertical shapes. The problem of structure was corrected when the fit of subtracting Monte Carlo data from nominal data.

2.2.4 Fitting the Differences

The other method for determining the fitting differences was to calculate the differences of the drift times followed by fitting the differences of data and Monte Carlo data into a plane rather than fitting the data sets *before* subtraction with Monte Carlo. Both methods are tested and compared. The reduced χ^2 functions of each method are computed to determine which method would produce the more reliable result.

2.3 Results

Looking at the Monte Carlo plots (Figure 11), the U slopes of the planes fluctuated between 0.5 and -1 ns/cm, and the V slopes of the planes fluctuated between 1 and -0.7 ns/cm. The trends of the Monte Carlo data are generally similar with the experimental data. The U slopes fluctuated between 1 and -2 ns/cm, and the V slopes between 1.5 and -2 ns/cm. All the data had overlapping values of slopes on each plane. The sloping on the planes that are roughly the same as Monte Carlo data, which means that there are no tilts into those planes since there cannot be any tilting in the Monte Carlo data. The slopes that are unlike the Monte Carlo may suggest that there was some tilting.

The effect of the bulge was clear in the plot of the fits' constant terms in both the U and V

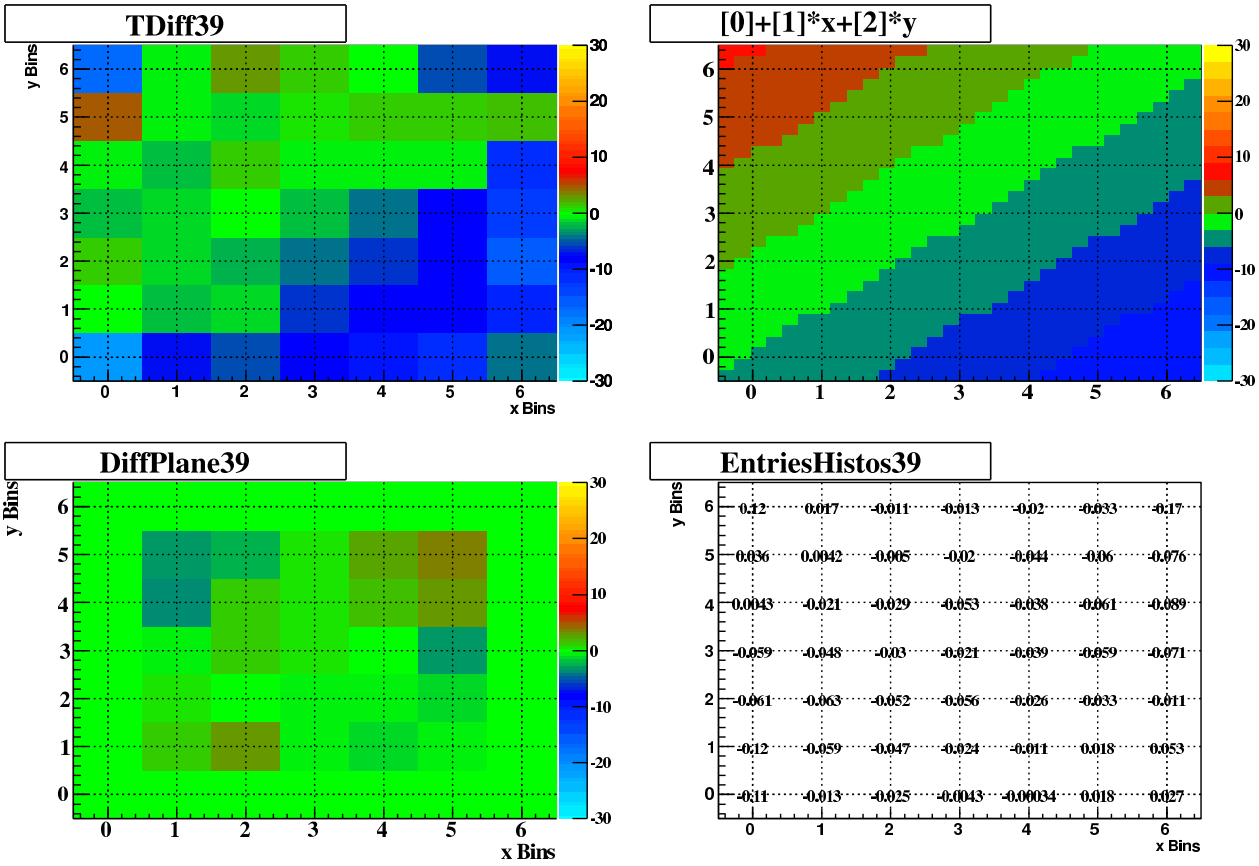

Figure 9: Sample plots for plane 39 in 107mT data.

planes. Figure 12 shows the expected offsets nicely. The diagram is meant to represent a plane in two conditions. The top case shows the expected effect of an increase in pressure (e.g. from 107 mT to 137mT). The foil of the plane would bulge "outward" allowing more space for the additional gas molecules. The bottom case in the figure shows the effect of a decrease in pressure like from 107mT to 77mT. The same foil surrounded by fewer gas molecules responds by reducing the volume in the plane's space. This is what is seen in the plots of the constant terms. The constants of the 137mT pressure are the largest, and those of the 77mT pressure are the smallest, with nominal 107mT and Monte Carlo 107mT located in the middle, as expected (Figures 13, 14). The constant terms clearly show the effect of pressure on the planes. The dense stack planes do not show a bulge.

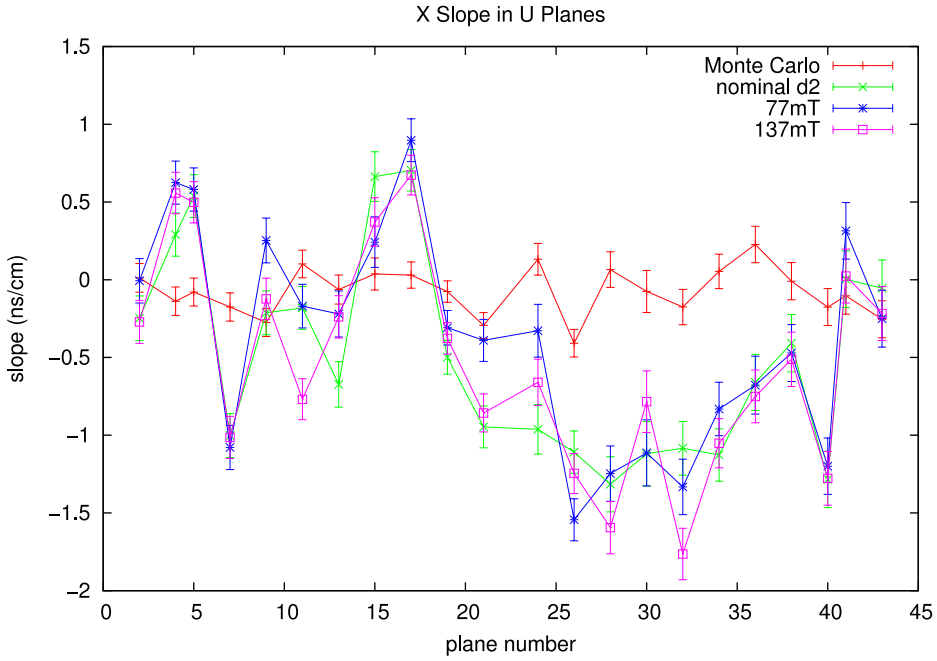

Figure 10: U slopes in the U planes for Monte Carlo data and the data sets analysed.

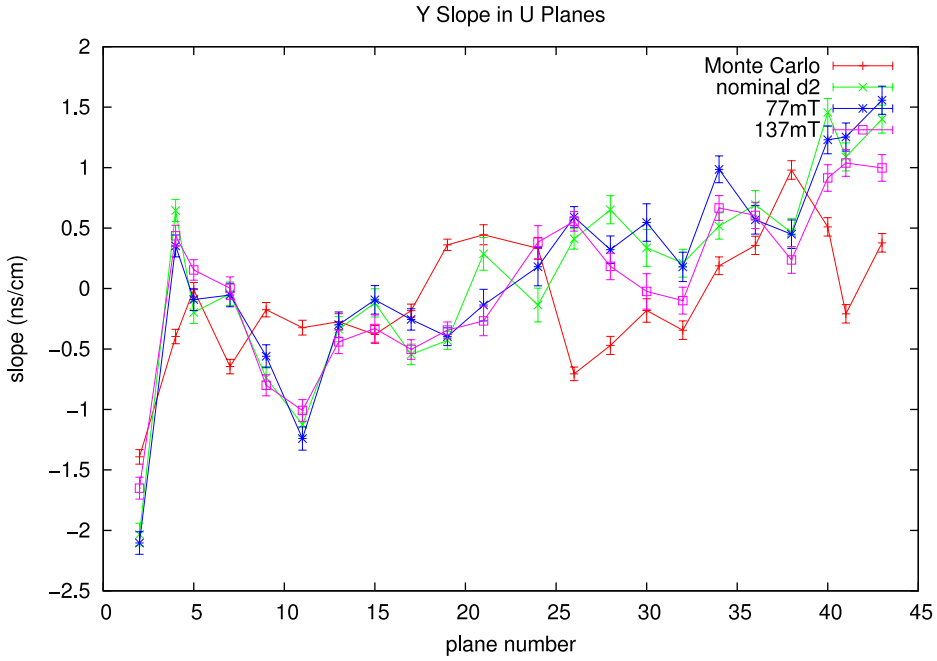

Figure 11: V slopes in the U planes for Monte Carlo data and the data sets analysed.

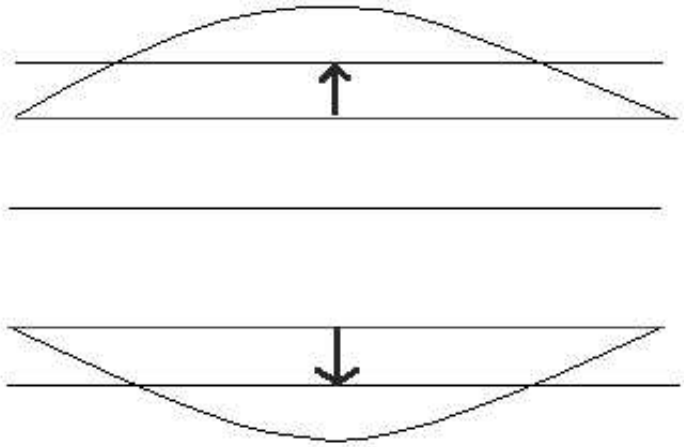

Figure 12: Effects of Pressure on a Foil

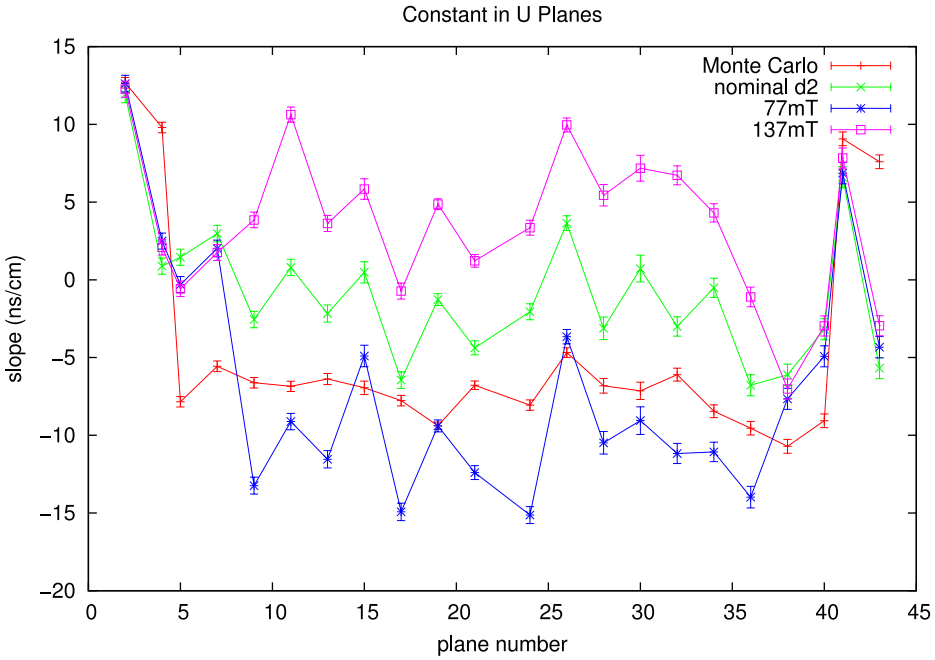

Figure 13: Fitted Constant Terms in the U Planes

Planes 21-24 are different in the way that they did not have a sloping tendency like the other planes. They are always more erratic, and their p0 pressures (the average pressure at which no bulging occurs) are inconsistent with the other planes. Usually, these planes are problematic in any detailed analysis of this kind. Jingliang reported a problem with the pressures of these planes in his posting but could not explain it. I am not sure why this is. The problem might be that because a decay only goes through two adjacent planes there is not as much information collected. Whereas in the dense stack, it goes through many planes giving more information. However, these planes are not used in calculating p0.

Similarly, the Z-asymmetry, the difference of the number of drift times on either side of the wire, was fitted to see if there was any slope present and also to see if there was any correlation with the U and V slopes of the fitted planes (Figure 15). This plot showed that the values are compatible with zero. There should not be much asymmetry since the cuts made both regions the same size. However, there was not any visible correlation of this asymmetry with the U slopes, V slopes, or the constants of the U and V planes.

2.3.1 Significance of the Reduced χ^2

The reduced χ^2s of the two fitting methods are analysed to judge whether the shape of the fit would be compatible with a planar fit in the first place. Interestingly, the method with the lowest χ^2 values was that of fitting the differences before calculating the fit. The comparisons can be seen in Figures 16 and 17.

Statistically, the closer the χ^2 value is to unity, the more reliable is the result. In these figures, the fit of the differences is closest to unity and the differences of the fits is furthest from it. Since getting the fit of the differences has the lowest χ^2 value, it is the most credible method. Also, because the slopes have values other than zero, there must be some tilting in the planes.

2.4 Directly Measured Gaps Between Planes

An analysis by Vladimir Selivanov was compared for compatibility with these results. He used a high-energy beam to directly measure the gaps between some wire planes and cathode planes. He measured offsets that would qualify as a kind of tilting [7].

Two of Vladimir's U and V axes are compatible with this analysis, and the other four axes are not. The geometry of the planes that Vladimir found are similar in structure to the incidence of drift

times found in this analysis. Figure 18 shows the comparison of the U axis of Vladimir's plane 37 (labeled V) with the U axis of the same plane for this analysis (labeled A). "V" is in microns and "A" is in nanoseconds. The "A" line was multiplied by a factor of 20 to better compare the trends. These measurements are not as compatible with Vladimir's results. Figure 19 shows the comparison of the V axis of Vladimir's plane 37 with the V axis of the same plane for this analysis. The lines are of the same units as in the previous U axis plot. The "A" line was also multiplied by a factor of 20. This comparison shows that the measurements are more compatible.

The difference in the analyses might have been because Vladimir's measurements are made on a bench. Other reasons for the differences could be that the planes might have been switched to new positions or rotated since the measurements are taken.

3 Conclusions and Future Use

There appeared to be tilting in the 2004 data that did not correspond to the tilts in the Monte Carlo data. This would suggest that there might be some real tilting in the planes.

It was concluded that region-dependent STRs, STRs that use several STRs per plane to account for temperature changes and field distortions, would be just as important as plane-dependent STRs, since the tilt changed for as much as the constant term. It is therefore necessary to further investigate the improvement from global driven STRs to region-dependent STRs [6].

It was found that individual planes have slightly different foil to wire distances. Ideally, when foils are parallel to each other, the plane-dependent STRs can be used. However, if there happens to be some tilting in the planes, then region-dependent would be necessary. This analysis might help to estimate the degree of largeness of the inter-plane-dependent results. To test the experimental data (or Monte Carlo data) for the amount of error without taking the tilt into account, one could implement a correction and use it to compare the results. With tilting, a linear correction to the drift times in U and V positions could be made before putting them back into the helix-fitter.

4 Acknowledgments

The writer would like to thank Drs Art Olin and Alex Grossheim for giving me the opportunity to learn about and contribute to the TWIST project at TRIUMF; and for their guidance and suggestions. I would also like to thank Anthony Hillairet for teaching me about the TWIST detector and helping me develop my code.

5 Appendices

5.1 Appendix A: Glossary

- Drift Chamber (DC): Obtains the "hit" or drift time of the particle while it travels through the chambers
- Helix-Fitter: Takes drift times from the DCs and comes up with the best trajectory that matches them.
- Monte Carlo data: Simulated data produced by GEANT3 to represent the behaviour of a particle [1].
- Proportional Chamber (PC): Gets the times to help with pattern recognition.
- Pressure of zero bulge (p0): The average pressure at which no bulging occurs [2].
- Plane-dependent STRs: One STR for each plane.
- Region-dependent STRs: Several STRs for each plane. They would come in handy for cases of temperature gradients or field distortions.
- Space-Time Relations (STRs): Relate the measured drift time to a position in the drift cell [5].
- TRIUMF Weak Interaction Symmetry Test (TWIST): measures the Michel (or muon decay) parameters that describe the energy and angle distributions of positrons from positive muon decay [5].

5.2 Appendix B: Additional Figures

5.2.1 Quality of Statistics

A natural concern about the analysis was that the quantity of statistics was affecting the outcome of the results. Generally, more statistics give more accurate results. A comparison was done in which four sets of data are plotted with 19 sets of data. Figure 20 shows that the slopes are compatible within errors, however the offset (constant) is not so compatible. For the remainder of the analysis, the data with 19 sets was used to take the most accurate data possible.

5.2.2 Data Analysis with Garfield

Another comparison that was done was to look at the differences between data taken from a Garfield program and data from data-driven STRs as in Figure 21. All other aspects of the analysis are done using data-driven STRs.

5.2.3 Upstream Stops Data

Similarly, other data using upstream stops, nominal target stop data to check for an improvement with this kind of data with the analysis. The plots of these comparisons are shown in Figures 22 through 27. Us19 and us20 are the labels for upstream, first iteration, and second iteration respectively. d2pd24 is the fourth iteration of plane dependent STRs. There is still some sloping/tilting visible in the plots that differ from nominal data. It is interesting that the constant terms have such a large gap between the nominal data and the upstream data. The gap may be somehow attributed to the helix fitter.

References

[1] Brun, R et al. (1995 April 3). *CERN Program Library Long Writeup W5013*.

<http://wwwasdoc.web.cern.ch/wwwasdoc/geant_html3/geantall.html>

Accessed 2007 Aug 30.

[2] Hillairet, A. (2007 March 14). *BulgeResults, 2006*.Private TWIST Collaboration Document. Accessed 2007 June.

[3] Hu, J. (2005 July 4). *Measurement of DC Module Geometry from Data*. Private TWIST Collaboration Document. Accessed 2007 June 24.

[4] Jamieson, B. (2005). *Measurement of the Muon Decay Asymmetry Parameter with the TWIST Spectrometer*. Vancouver, BC: University of British Columbia.

[5] Marshall, G. (2006). *TWIST: Research Proposal*. <https://twist.triumf.ca/> Accessed 2007 Aug 27.

[6] Mischke, R. (2007 August 3). *Assessing the Need for Region-Dependent STRs*. Private TWIST Collaboration Document. Accessed 2007 August 4.

[7] Selivanov, V. (2007 June 22). *About Obtaining of Correct STR and Resolution for DC4 of the TWIST Detector*. Private TWIST Collaboration Document. Accessed 2007 June 22.

[8] TRIUMF. (2007). *TWIST*. <twist.triumf.ca> Accessed 2007 July 13.

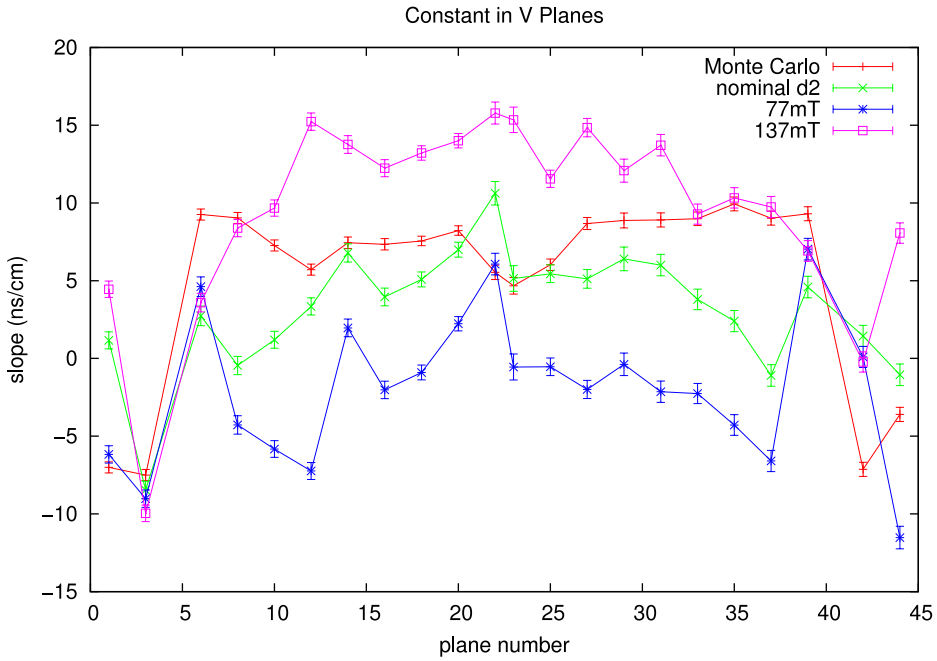

Figure 14: Fitted Constant Terms in the V Planes.

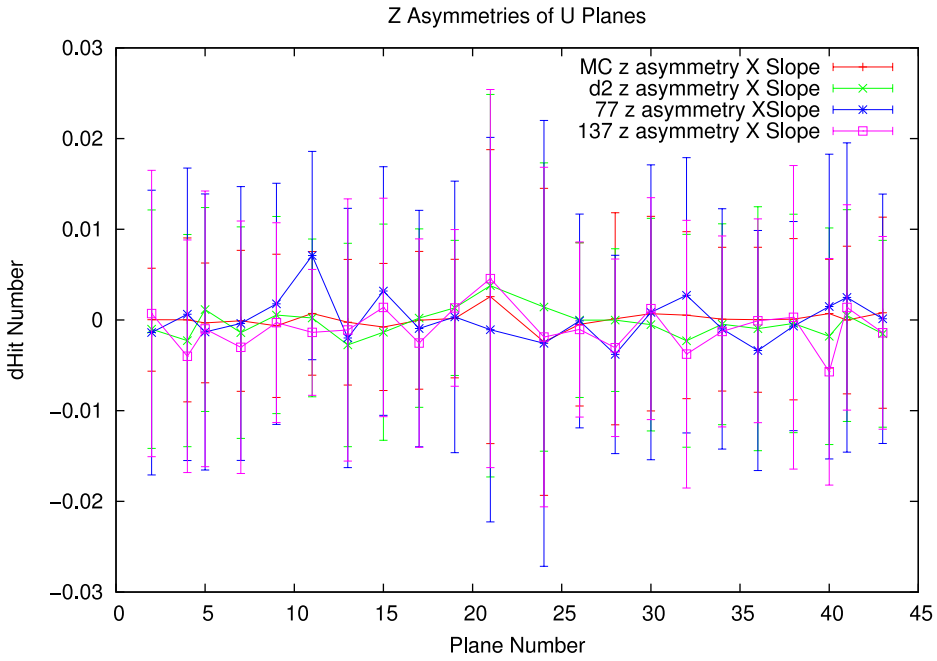

Figure 15: Differences of numbers of drift times on sides of the wire

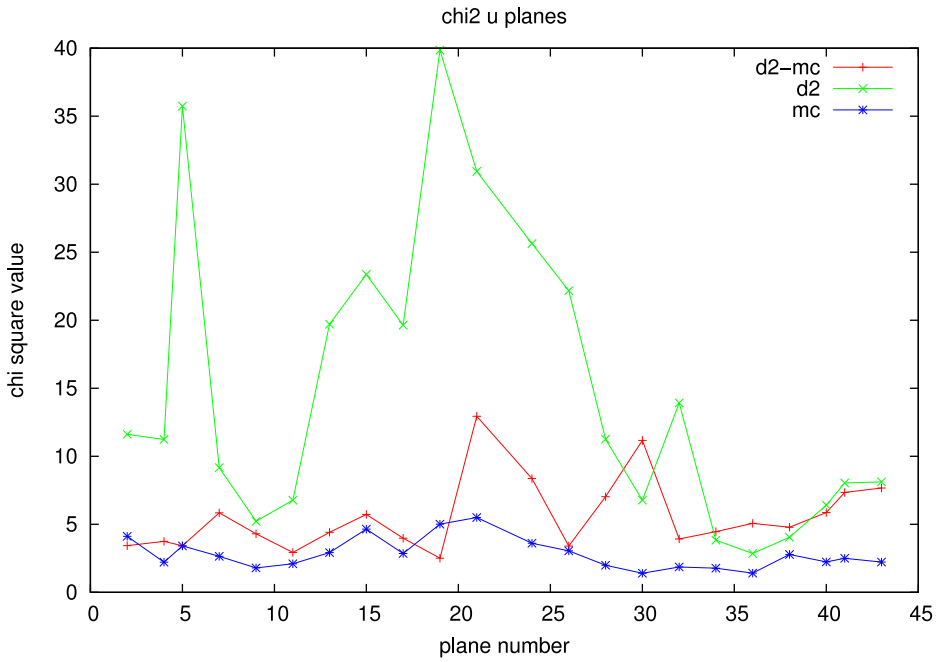

Figure 16: χ^2 Analysis in U Planes.

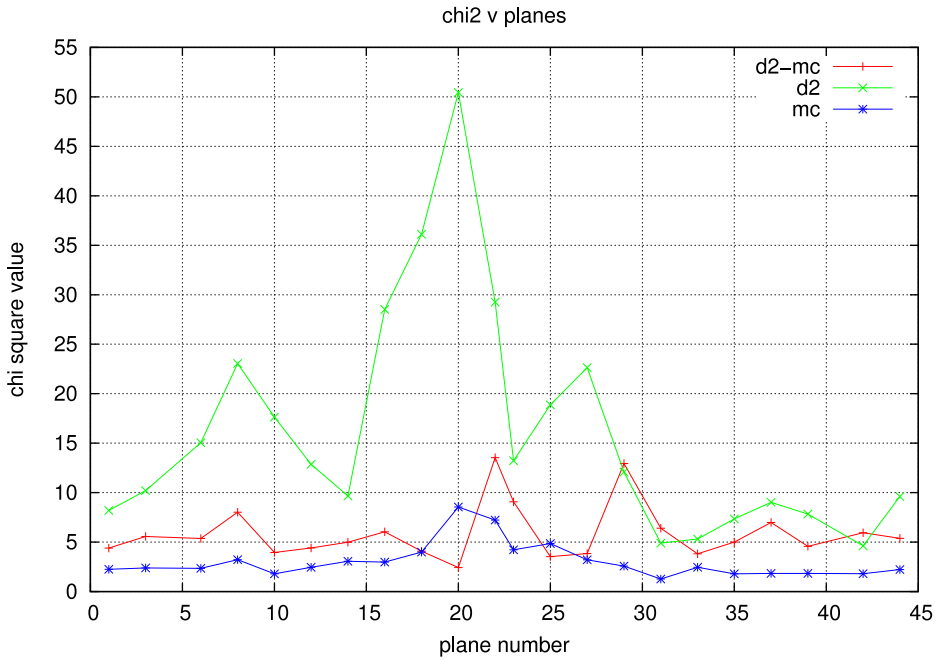

Figure 17: χ^2 Analysis in V Planes

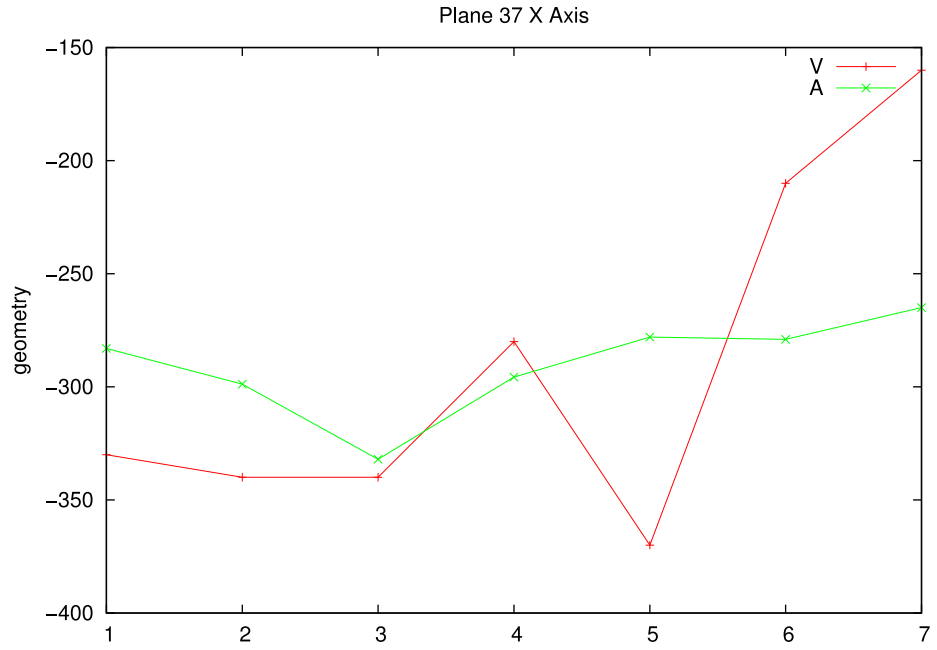

Figure 18: Comparison of the U axis of plane 37 for the two analyses.

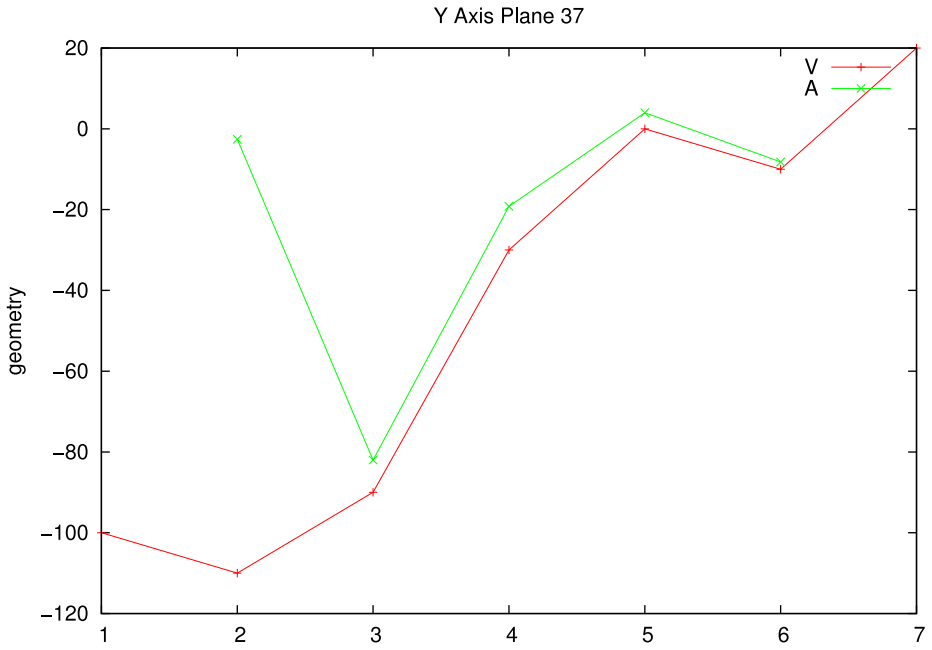

Figure 19: Comparison of the V axis of plane 37 for the two analyses.

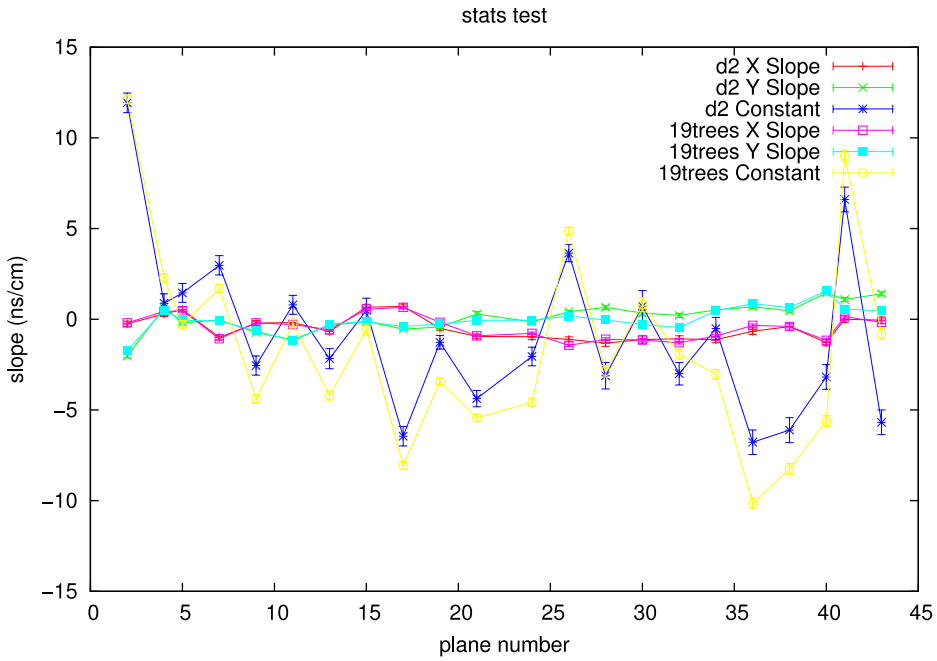

Figure 20: Quality of Statistics

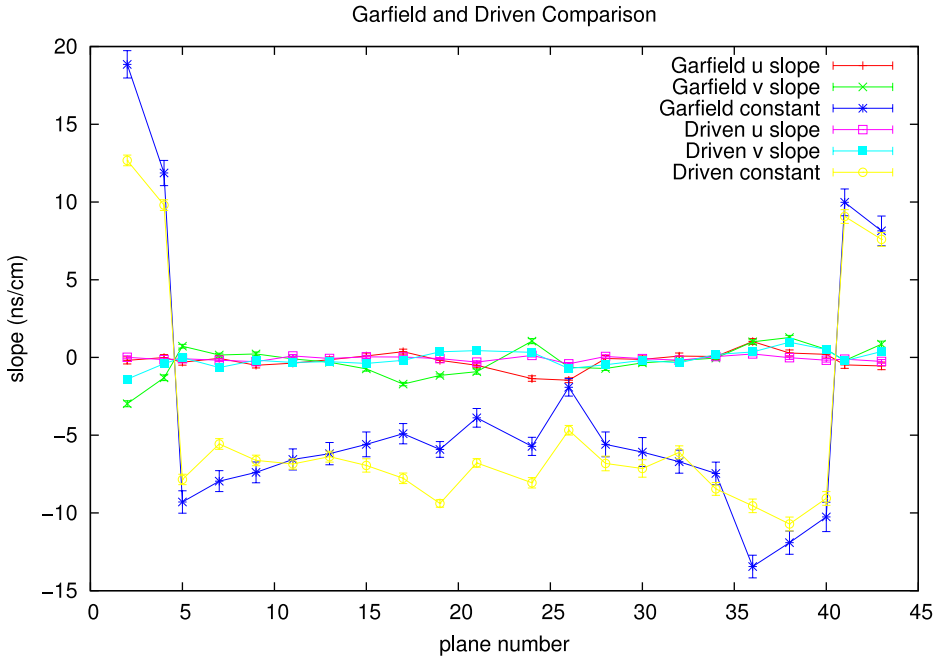

Figure 21: Garfield and Driven Monte Carlo Data.

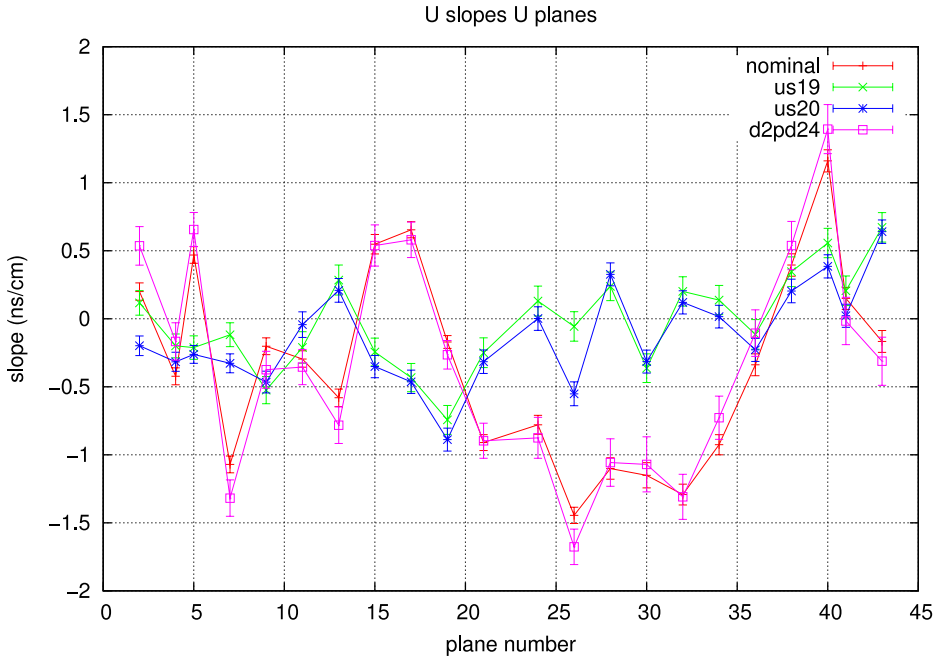

Figure 22: Upstream stops and nominal data; U slopes in U planes.

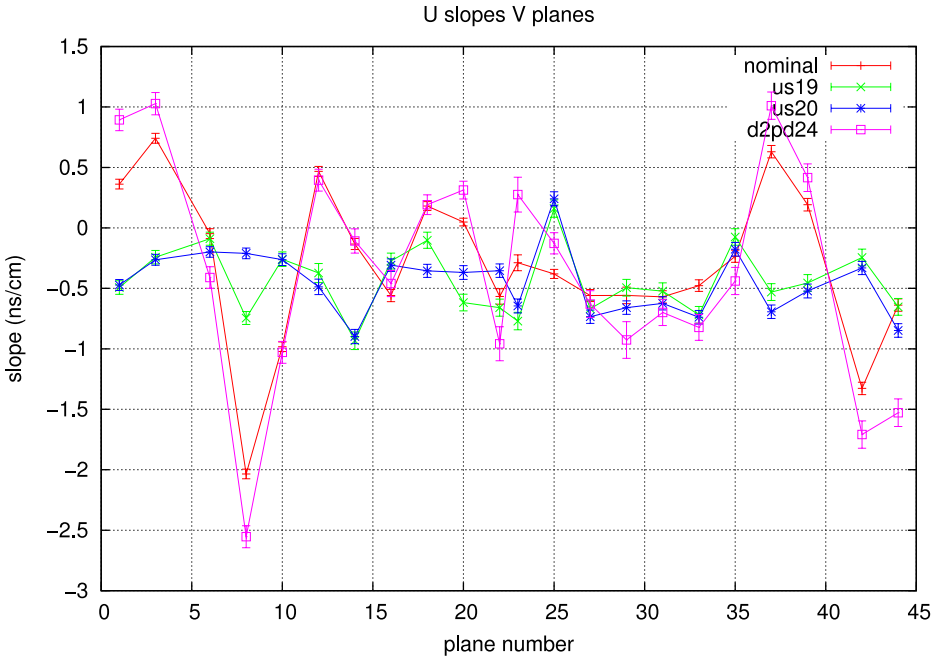

Figure 23: Upstream stops and nominal data; U slopes in V planes.

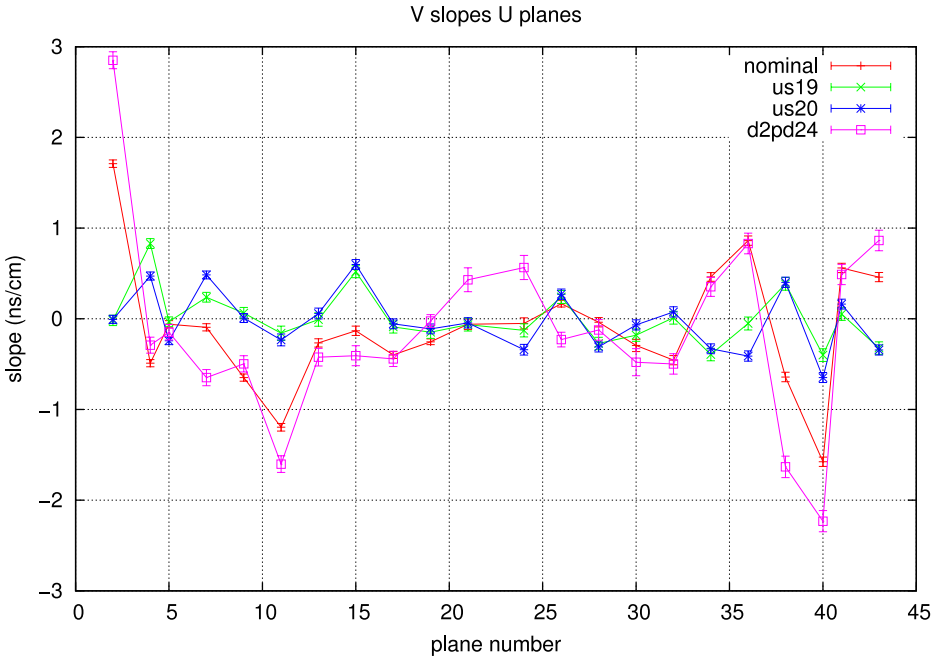

Figure 24: Upstream stops and nominal data; V slopes in U planes.

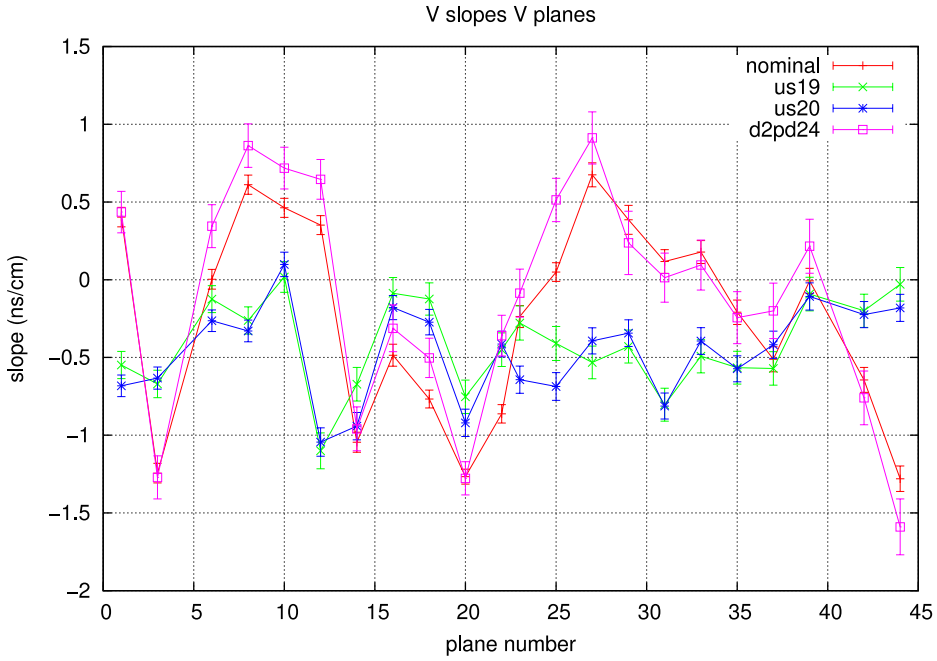

Figure 25: Upstream stops and nominal data; V slopes in V planes.

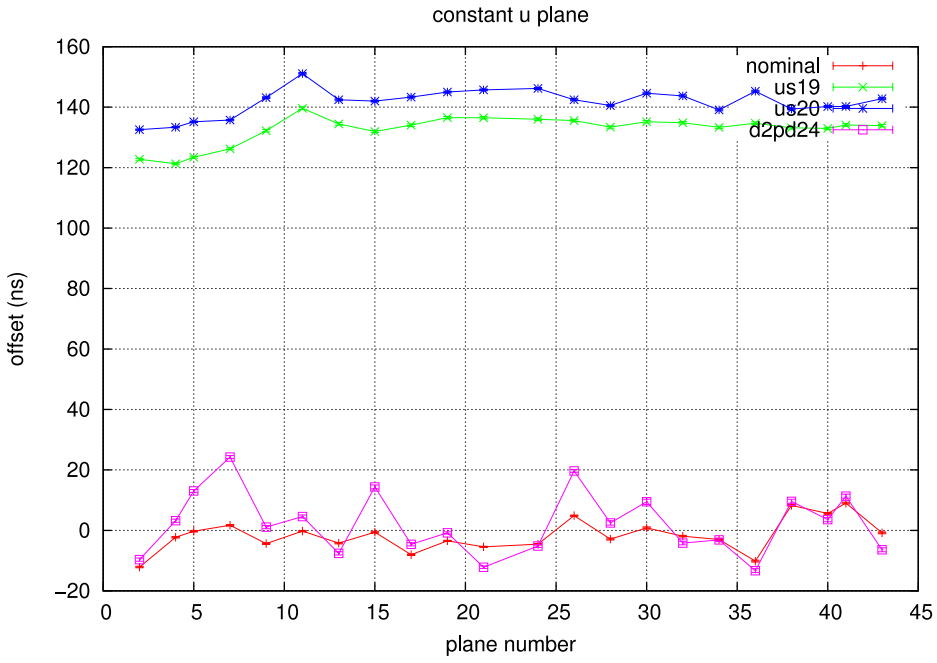

Figure 26: Upstream stops and nominal data; Constants in U planes.

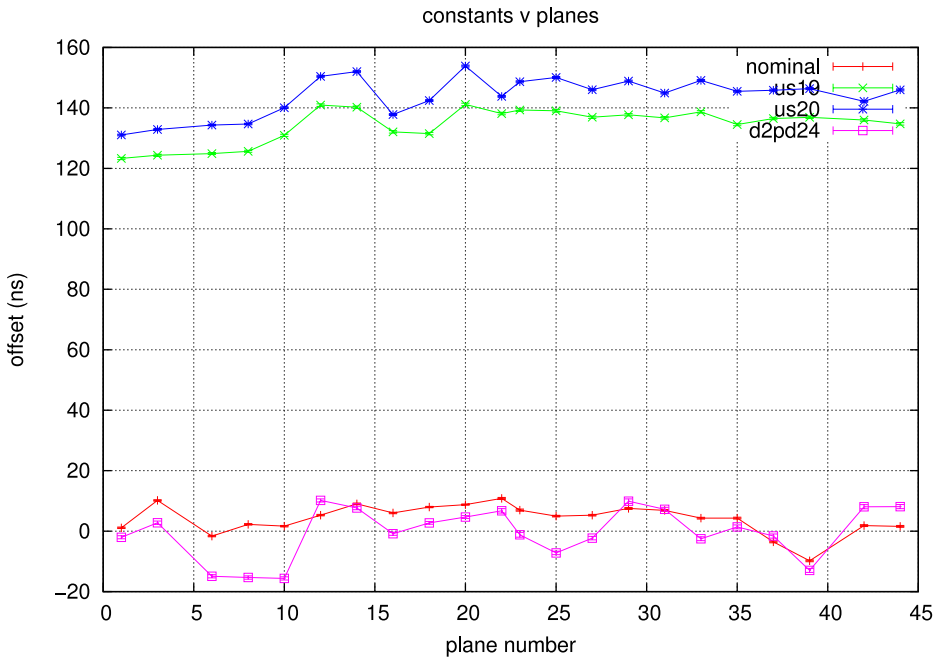

Figure 27: Upstream stops and nominal data; Constants in V planes.